



The effects of scale-up and coal-biomass blending on supercritical coal oxy-combustion power plants

R. López^{a,*}, M. Menéndez^b, C. Fernández^a, A. Bernardo-Sánchez^b

^a Department of Chemical Engineering, University of León, León, 24071, Spain

^b Department of Mining Technology, Topography and Structures, University of León, León, 24071, Spain

ARTICLE INFO

Article history:

Received 9 April 2017

Received in revised form 28 January 2018

Accepted 30 January 2018

Available online xxx

Keywords:

Oxy-combustion

Bio-CCS

Economic analysis

Scale-up

Biomass blends

ABSTRACT

Carbon Capture and Storage (CCS) with biomass is called to be one of the most important technologies to reduce the climate change all over the world. In addition, supercritical pulverized coal plants have been pointed out as interesting power installations because its high efficiency. In this work, the effects of plants scaling and biomass-coal co-firing level on net present value (NPV), cost of energy (COE) and cost of CO₂ avoided (CCA) have been studied on a supercritical pulverized combustions coal/biomass blends. Aspen Plus[®] was used to implement technical simulations. Finally, the main factors affecting plants viability were identified by a sensitivity analysis. The results obtained revealed that the use of biomass reduces the NPV in (−0.23, −1.75) M€/MWe, and increases the COE by (0.007, 0.263) M€/MWe. However, plant scaling was found to be a more important factor, by reaching an impact of 4.32 M€/MWe on NPV variation in best case. The reduction of oxy-plants viability by biomass using as raw material could be compensated by an increasing of the designed scale-up. Finally, 300 MWe power plants with 40–50% biomass co-firing level were identified as a compromise solution between economy and risk, improving in this way the interest for potential investment.

© 2017.

Abbreviations (in order of appearance on text)

UNFCCC	United Nations Framework Convention on Climate Change
WMO	World Meteorological Organization
UNEP	United Nations Environment Programme
IEA	International Energy Agency
OECD	Organization for Economic Co-operation and Development
CCS	Carbon Capture and Storage
NPV	Net Present Value
COE	Cost Of Electricity
CCA	Cost of CO ₂ Avoided
RYIELD	Aspen tool used to simulate reactions with established yields
RGIBBS	Aspen tool used to simulate reactions when free Gibbs energy is minimised
ASU	Air Separation Unit
DESOX	Desulfurization Unit
TEC	Total Equipment Costs
NETL	National Energy Technology Laboratory (U.S. Department of Energy)
CEPCI	Chemical Engineering Plant Cost Index
FCI	Fixed Capital Investment

TCI	Total Capital Investment
EBTF	European Benchmarking Task Force
NREL	National Renewable Energy Laboratory (U.S. Department of Energy)

1. Introduction

In the new global economy, climate change has become a central issue for the international community. It is becoming increasingly difficult to ignore the important role of the connection between the science community, party and non-party stakeholders to benefit the intergovernmental process and Paris Agreement implementation. In order to improve this work, the last Earth Information Day was organised by the UNFCCC and celebrated in Casablanca on last November. In that conference, 2015 was presented as the warmest year, over 1 °C higher than pre-industrial period [1] by the WMO. According with this finding, the concentration of long-lived greenhouse gases continues to increase, reaching in 2015 the world mean value of 400 ppm (CO₂), 1845 ppb (CH₄) and 328 ppb (N₂O). A considerable amount of literature has been published on the consequences of this situation, such as a record warming at ocean surface and subsurface, the rising on sea levels or more irregular precipitations (very dry in some places and wet in others) [1,2]. In addition, high impact extremes have been attributed to the climate change: 7800 deaths in the Philippines attributed to Typhoon Haiyan, 2013; 250000 excess deaths attributed to drought and famine in 2011–2012 in the Horn of Africa or 4100 deaths attributed to heatwaves in Pakistan and India in

* Corresponding author.

Email address: rlopg@unileon.es (R. López)

2015 [2]. The causes of this situation must be identified in order to avoid higher disasters.

Many authors have identified the principal cause with the increasing of energy demand due to the economic development and the population growth. The IEA expects a continuous rising on energy demand of OECD countries from 5500 Mtoe in last 2014 for the next 25 years. In addition, developing countries and regions, such as China, India, South and Central America and the Middle East are expecting to be the main sources of the energy demand increasing in that time. In addition, some geopolitical uncertainties in Middle East countries have established increasing concerns about the future oil supply. In Europe, the recent United Kingdom decision about leaving the European Union has no precedents in Europe uncertainties.

In this international context, the European Commission established the Directive 2009/28/EC of the European Parliament and of the Council of 23 April 2009 on the promotion of the use of energy from renewable sources [3]. All the while, it was published the Decision No 406/2009/EC of the European Parliament and of the Council of 23 April 2009 with the objective of reduce the EU States greenhouse gas releases in a time frame of 10 years, up to 2020. Therefore, a 2011–2020 Renewable Energies Plan was designed by the Spanish Energy Department [4] to increase the energy pool production by green energies by a minimum of 20% in 2020. Recently, the European Union approved the programme Horizon 2020 as the European Investigation and Innovation Framework Programme in the same field.

A considerable amount of literature has been published about different technologies to reduce greenhouse gases emissions [2,5,6]. Between them, carbon-based combustion with CO₂ capture has revealed to be one of the most interesting one for reducing the anthropogenic CO₂ emissions [7]. CCS has been considered a promising solution because: (1) anthropogenic global climate change is a serious problem and (2) there is a need for large reductions in carbon dioxide (CO₂) emissions [8]. Between the different CCS technologies, oxy-combustion can be established as a valid solution due to it can be used as a CO₂ sink, reducing the greenhouse gases environment effects. Oxy-combustion processes are characterised by burning fuel in an atmosphere composed by a mixture of CO₂ and O₂ [9]. After combustion, flue gases are partially returned to the combustor stream feed in order to control the flame temperature [10]. The Spanish Renewable Energies Plan established the objective of designing CCS plants with, at least, 40% efficiency from 2017 to make CCS plants cost competitive since 2020.

Supercritical power plants are expected to be one of the possible solutions to increase the CCS efficiency that Spanish Renewable Energies Project considers [11].

Many raw materials have been used as oxy-combustion feedstock. Between them, biomass is a suitable bioresidue for being used in waste combustors to generate high enthalpy steam, good for producing electricity. Biomass is also called to modify the carbon balance of different energy processes from positive (fossil fuels) to neutral or negative (Bio-energy with CCS, also called Bio-CCS) [5].

In previous works, several biomasses oxy-combustion were analysed and biomasses were selected based on their oxy-combusting behaviour [12]. After selection, the oxy-combustion experimental conditions were optimized and the transport phenomena occurring in the particles during oxy-combustion was studied by the application of the conservation equations [10].

The present study was designed to determine the effect of the power size escalation and the biomass with coal co-firing level on the economic viability of a supercritical oxy-combustion power plant. This study was performed by assessing the NPV, COE and CCA

variation for five proposed biomass co-firing levels: 0%, 15%, 25%, 50% and 100%. In addition, these levels were combined with different gross electric energy production: 140 MWe, 300 MWe and 460 MWe. These gross power productions were in accordance with Stanger et al. [13] works when they stated: “oxy power plants with CO₂ capture to be built should have capacities in the range of 100–500 MWe (gross)”. The conclusions obtained by the evaluation of the fifteen proposed scenarios added to a growing body of literature on oxy-combustion technology and were considered useful to improve several alternative processes to traditional electric production by only coal combustion.

2. Materials and methods

2.1. Materials

Two raw materials were used in this study: a bituminous coal obtained from the northern located mines of León (Spain) and a lignocellulosic biomass blend used in previous works [14]. The biomass was delivered from the north of Spain. The biomass blend proportion was established in 70% rape vs. 30% corn according to best oxy-combustion results (pending publication). It was taken as a field bioresidue. The procedures used in biomass characterisation were described in previous works [10]. However, the same properties values in the bituminous coal case were obtained from the data project of a power plant with the same coal as main feedstock [15].

Table 1 summarised the physical and chemical properties of raw materials used in simulations.

2.2. Methodology

Fig. 1 showed the three parts in which the techno-economic study was divided. Fifteen scenarios were considered by modifying the proportion of biomass on the oxy-combustor feed and the gross output power obtained in the power plant turbines. Five different biomass co-firing levels (0%, 15%, 25%, 50% and 100%) were combined with the three proposed gross powers (140 MWe, 300 MWe and 460 MWe) by the assumption of a constant heat input [16].

By implementing Aspen Plus[®] simulations, the main thermal and power values of each block and stream of the flowsheet were ob-

Table 1
Physical and chemical properties of raw materials used in simulations.

Material	Coal	Biomass
Proximate analysis		
Moisture (%)	12.0	10.1
Volatile matter ^a (%)	32.0	52.4
Ash ^a (%)	25.5	14.4
Fixed carbon ^{a,c} (%)	30.5	23.1
Ultimate analysis		
C ^b (%)	65.1	57.3
H ^b (%)	2.9	4.6
N ^b (%)	1.4	0.8
S ^b (%)	1.9	1.0
O ^{b,c} (%)	28.7	36.3
Calorific value		
HHV (MJ/kg)	25.08	19.18
Properties		
Grindability index	50	27
Dielectric constant	5.0	2.5

HHV_—high heating value

^a Dry basis.

^b Dry ash free basis.

^c Calculated by difference.

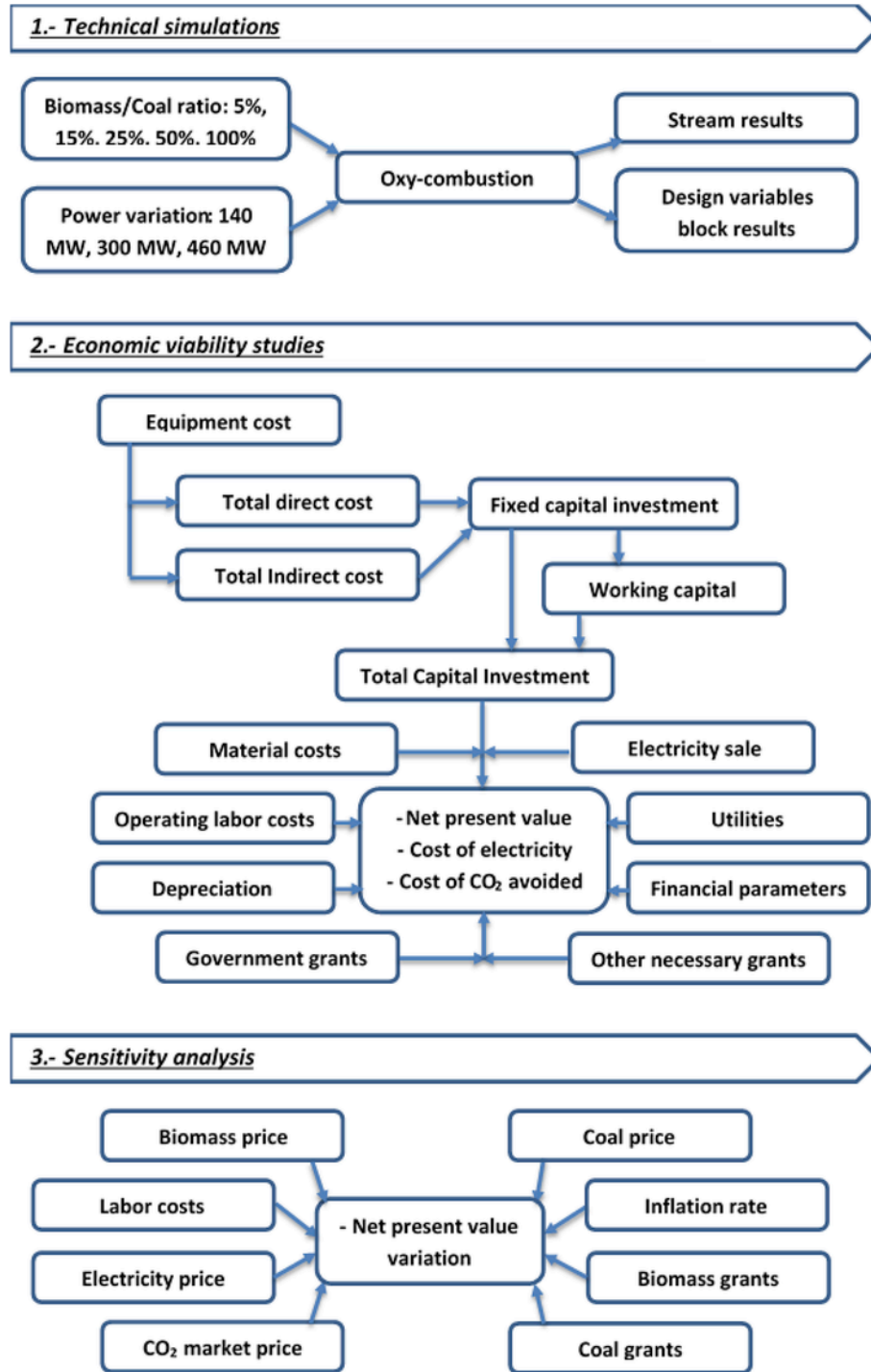


Fig. 1. Techno-economic analysis scheme methodology.

tained. The thermodynamic model was based on the Peng-Robinson with Boston-Mathias modifications property method. Peng-Robinson equation of state was previously used by other authors [17] with positive results.

Afterwards, a viability study was performed for each scenario by evaluating the behaviour of NPV, COE and CCA. The objective of this economic study was to make a comparison of the power plants economy previously simulated, taking into account the different raw materials and gross power points of view.

Finally, due to the instability of several variables affecting to the economic viability of the power plants, a sensitivity analysis of a selected co-firing level of 50% for each gross power production was performed.

2.2.1. On the technical simulations

The general considered assumptions in simulations were, as follows: (1) the blocks parameters were considered in stable state, (2) no diffusional effects were taken into account in combustor, and (3) in

oxy-combustion modelling, H, O, N, S were volatilized, C was converted to pure coke and ash was not considered as a reacting lump.

All scenarios were simulated using a flowsheet based on previous works [18,19]. In order to clarify the simulations descriptions, flowsheet was divided into two different parts: (1) the combustor and auxiliary equipment process, and (2) the Rankine water cycle process. The combustor and auxiliary equipment process was shown in Fig. 2. This figure was divided into two other representations. Fig. 2 a. showed a blocks diagram of the process. Air and different feedstocks were considered as main material inputs in the system, while dust, gypsum and CO₂ for storage were the main output material streams. Different plant zones were taken into account: O₂ preparation, feedstock preparation, combustor, flue gas treatment and Rankine cycle. Heat and materials connections of equipment in the combustor and auxiliary equipment process were shown in Fig. 2 b.

Raw materials, coal and biomass in the proportion of the respective run, were supplied at 4–6 cm (25%), 6–8 cm (55%) and 8–10 cm (20%) at 25 °C and 101,3 kPa. Both coal and biomass were dried (FD) with a previously heated (NH) nitrogen flow. Afterwards, they were fed into a crusher (CR) in order to reduce the particle size to 100 μm before being introduced to the combustor. The combustion was simulated as follows: firstly, solids were split into its composition elements in a RYIEDL block (RYIELD). The mathematical model was based on the definition of yields of different raw materials to gases reactions. Yields were defined in mass basis with the information provided in Table 1. The decomposition products were C, H₂, O₂, N₂, S and ash. Finally, the RGIBBS block (RGIBBS) simulated the oxidation reactions of the previously devolatilized components with a gas stream heated just before. The RGIBBS unit modelled reactions that come to chemical equilibrium by minimizing the Gibbs free energy of system [20].

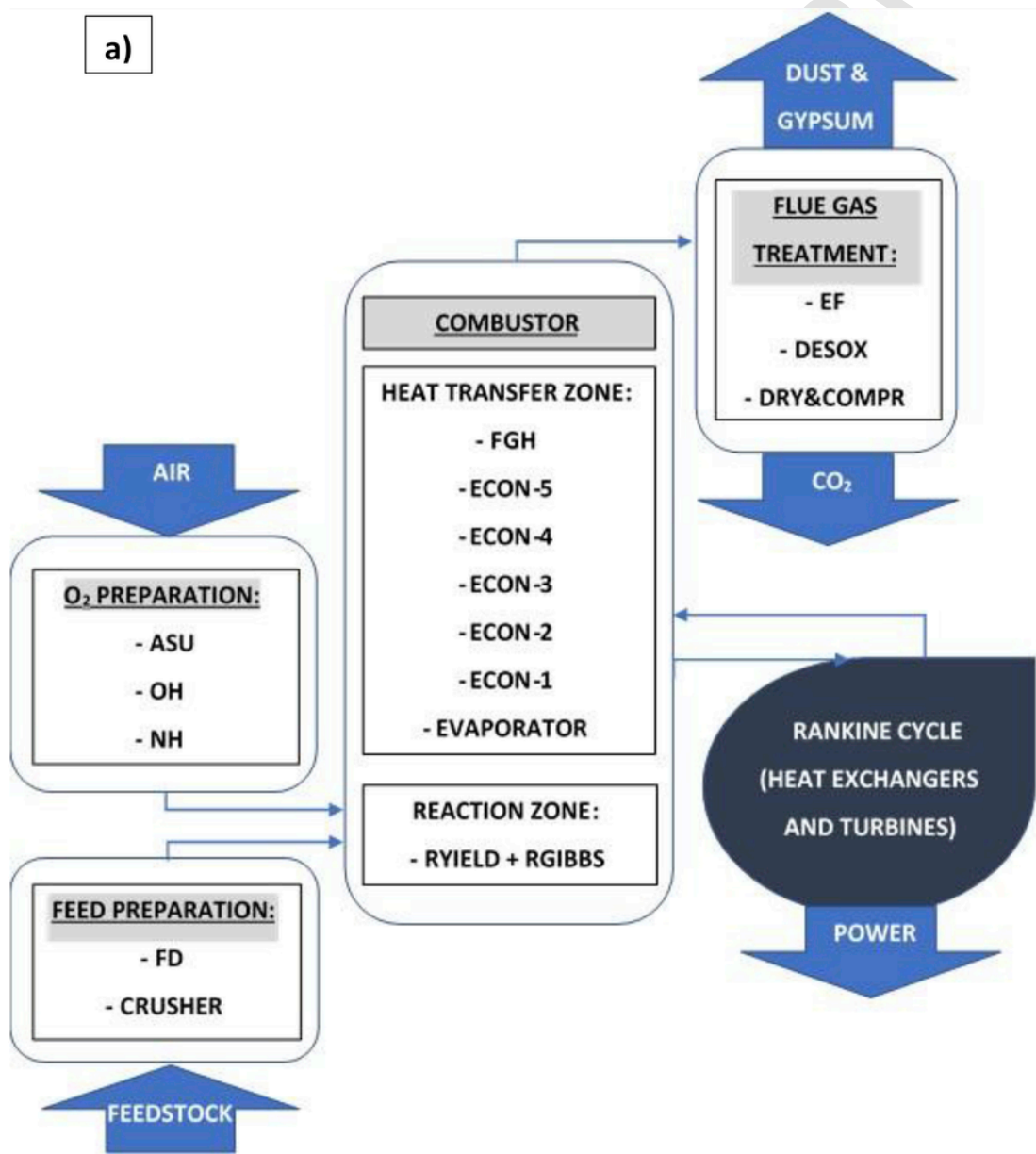


Fig. 2. a) Blocks diagram of power plants process, b) Combustor and auxiliary equipment process flowsheet.

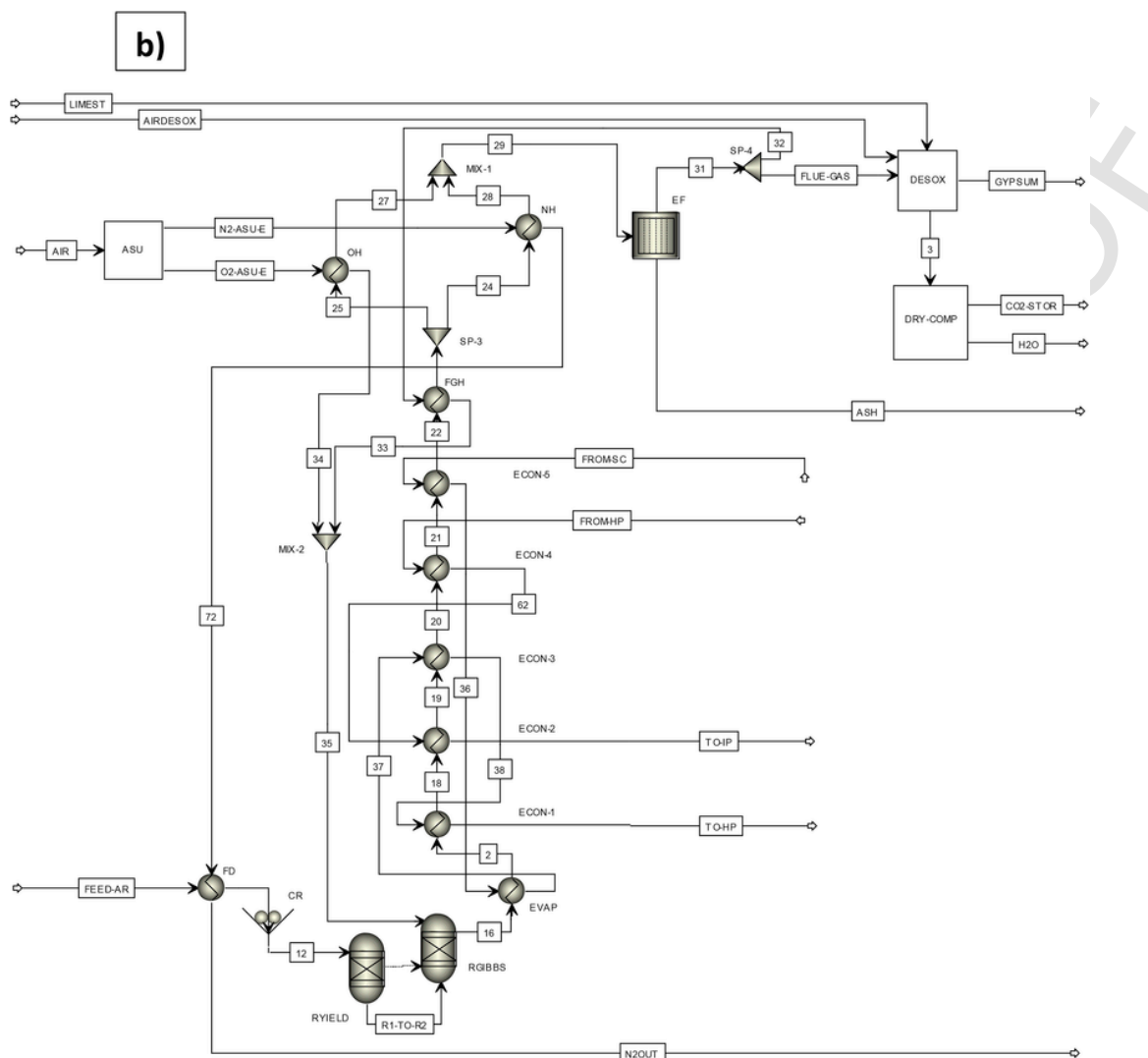


Fig. 2. (Continued)

The gas flow previously heated was composed by the CO_2 recirculated from the exit of the electrostatic precipitator and the O_2 produced in the ASU. A cryogenic ASU was selected [21] to separate air mainly components due to the high O_2 needs. The N_2 was discharged to the environment. The CO_2 stream was heated in a fuel gas heater (FGH) with the combustion gases as much as possible (hot/cold outlet temperature approach of 2°C).

The oxygen stream was 30°C heated in an oxygen heater (OH). Both, the CO_2 and O_2 streams were mixed in a $\text{CO}_2:\text{O}_2$ mole rate of 2.7 (results pending publication [13]) and introduced directly in the RGIBBS block. A heat stream connected the RYIEDL block to the RGIBBS block in order to consider the decomposition of raw material heat reaction in the combustor enthalpy balance. For the purpose of obtaining a high efficiency, a wet flue gas recirculation was chosen as it has been previously justified [19]. Afterwards, the water of Rankine cycle was evaporated by using the heat of flue combustion gases in an evaporator (EVAP). The evaporator produced a high enthalpy steam stream (207°C , 29MPa). This water stream was previously preheated in another heat exchanger (ECON-5) by cooling the exhaust combustor gases in 55°C . Once the steam was generated, it was reheated in two stages: firstly, a heater (ECON-3) was used to

rise the temperature until 350°C . Secondly, another heater (ECON-1) was used to produce a supercritical steam of 600°C just previously to be fed to the high pressure multistage turbine. The combustion gases heat integration was completed with two additional reheaters. ECON-4 was used to heat a steam stream from the high pressure multistage turbine until 600°C . Afterwards, this stream was fed to another heater (ECON-2) reaching a steam outlet temperature of 625°C previously to be fed to the intermediate pressure multistage turbine.

Once the heat of combustion gases was recovered as much as possible, exhaust combustion gases were cleaned in accordance with the Directive/75/EU of the European Parliament and of the Council of 24 November 2010 on industrial emissions [3] and the Royal Decree-Law of the Spanish Government No 1/2016, of 16th December, of integrated pollution prevention and control [4]. Firstly, combustion ashes were separated by an electrostatic precipitator (EF). Secondly, a DeSOx unit was used to reduce the SOx gases by a gypsum transformation using limestone as feedstock. Finally, due to the main composition of oxy-combustion gases, CO_2 and H_2O , a Dry & Compression unit was used to make water condense and to obtain an output stream of CO_2 with a higher purity than 98% ready to storage [22,23].

The Rankine water cycle process was presented in Fig. 3. The cycle was mainly designed by three multistage turbines, a condenser, a water pump and several heat exchangers in order to complete the heat integration system. The supercritical steam stream from ECON-1 was connected to a high pressure multistage turbine (HP). In the first stage, the steam was expanded to 8.2 MPa. In the last stage, the output of the turbine was set at 5.1 MPa. The steam at 8.2 MPa was used to preheat the water of the cycle by rising the water in 30 °C in a heat exchanger (HHR3). At last, a fraction of the turbine steam output was also used for the same proposal, rising water temperature in 37 °C in another heat exchanger (HHR2). Both steam streams were mixed with a lateral output of the intermediate multistage turbine (IP) and they were all fed to another water heater (HHR1) in which water was heated other 30 °C. Hot stream outlet was afterwards introduced to the deaerator system (DEA). The other stream fraction of the outlet of the high pressure turbine was sent to the combustor area in order to be reheated in both ECON-4 and ECON-2 before it was fed to the intermediate pressure multistage turbine (IP). This turbine was designed with three stages with discharge pressures of 2.8 MPa, 1.2 MPa and 0.5 MPa. The first stream was directly connected to the deaerator. The second stream was used to preheat the water flow in a heat exchanger (SC) in 10 °C before it was sent to ECON-5. Finally, the third stream was divide into two substreams. One of them was used to preheat the water stream in LHR4 by 30 °C. The other substream was fed to the low pressure multistage turbine (LP). This turbine was designed with four stages with discharge pressures of 0.2 MPa, 0.09 MPa, 0.03 MPa and 0.01 MPa. The first, second and third outlet streams were used to preheat the water stream in LHR3, LHR2 and LHR1 by 30 °C in each respectively. The last discharge stream was fed to a condenser (CND) in order to obtain liquid water at 32 °C. This condenser was used to know the heat exchanged in the equipment and, in economic calculations, a refrigeration tower was considered. Afterwards, the water was pumped (CP) with a discharge pressure of 1.6 MPa before it crossed LHR1, LHR2, LHR3 and LHR4 towards the deaerator, rising its temperature. Finally, a water stream was obtained in the deaerator and it was connected to another pump (FWP) to increase the pressure to 29 MPa again. This water was preheated in HHR1, HHR2, HHR3 and SC as a previous operation before it was fed to ECON-5 in the combustor area. Isentropic efficiencies were set at: 0.85 (pumps), 0.90 (HP), 0.92 (IP) and 0.86 (LP) [24].

A design spec was performed with the total power production as the specified variable. The values varied between 460 MWe, 300 MWe or 140 MWe (calculated as the contribution of the three multistage turbines). The design spec was completed by defining the water Rankine flow at the deaerator exit as the manipulated variable. The default convergence methods were set as: Wegstein for tears solving and secant for single design spec resolution. When tears and design spec were necessary to solve together, Broyden method was used. In all cases, the maximum objective and residual tolerances in iterations were set at 1E-6. In calculations, the maximum errors of main variables were as follows: 1E-5 K for temperatures, 1E-7 for mass flows calculations and 1E-6 for pressure values.

2.2.2. On the economic viability studies

The aim of these studies was to obtain the NPV, COE and CCA. Firstly, TEC was obtained. Individual plant component cost was calculated by considering one equipment representative variable (for example, total power for turbines). Prices were taken over from the NETL publications [22,23,25]. Finally, the representative variable was used to obtain the actual cost C by a known reference cost C_0 component with a size S_0 by the following expression [6]:

$$C [M\text{€}] = C_0 \left[\frac{S}{nS_0} \right]^f \quad (1)$$

where S is the actual size and f is the scale factor (0.7 by default).

Prices used were published in 2011, 2015 or 2016, depending on the used source. 2016 prices were not modified, but 2011 and 2015 prices were updated in combination with the newest CEPCI values. Equipment costs were obtained individually with this methodology except those of ASU, DeSOx, Dry & Compression of CO₂ and combustor, evaporators and fuel dryer units costs. In these cases, all unit cost was obtained as a single value for the unit as a whole (for example, the water of Rankine cycle evaporated in combustor unit [22,23]).

FCI was calculated as the sum of the total direct and indirect costs. Peters et al. [26] proposed a calculation procedure based on the purchased equipment cost by using a proportional TEC factor. These factors were shown in Table 2. Afterwards, the working capital was

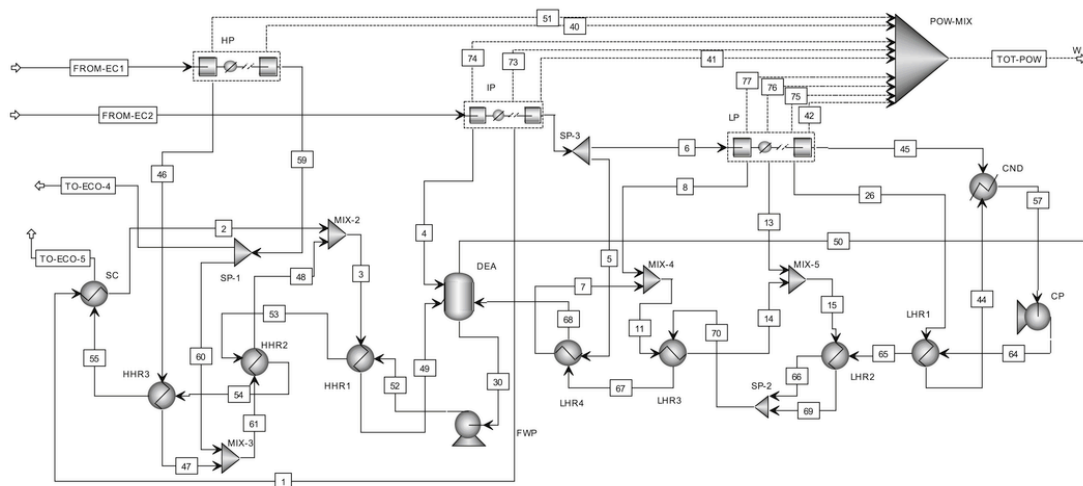


Fig. 3. Rankine water cycle process flowsheet.

Table 2
Peters coefficients used in economic calculations.

Factor		Coefficient
Direct costs		
Equipment delivery	Fraction of TEC	0.10
Purchased equipment installation	Fraction of TEC	0.39
Instrumentation and control (installed)	Fraction of TEC	0.26
Piping (installed)	Fraction of TEC	0.31
Electrical systems (installed)	Fraction of TEC	0.10
Buildings (including services)	Fraction of TEC	0.29
Yard improvements	Fraction of TEC	0.12
Service facilities (installed)	Fraction of TEC	0.55
Indirect costs		
Engineering and supervision	Fraction of TEC	0.32
Construction expenses	Fraction of TEC	0.34
Legal expenses	Fraction of TEC	0.04
Contractor's fee	Fraction of TEC	0.19
Contingency	Fraction of TEC	0.37
Working capital	Fraction of TEC	0.75

estimated by the 75% of TEC. Finally, the TCI was obtained by adding the FCI and the working capital.

The material costs, the electricity sale, the operating labour costs, the utilities costs, the plants linear depreciation, the financial parameters and the public grants were the main considered factors to calculate the economic indicators (NPV, COE, CCA).

At last, technical simulations results and 2016 Spanish markets prices were used to obtain the utilities costs.

Table 3 showed the main considered assumptions taken into account in the viability study. Spanish markets were the source at which electricity and raw material costs were obtained [4]. The inflation rate was in accordance with last years values [27]. The labour costs were obtained by considering the following employees: 1) Single shift: one plant manager, one fuel procurement specialist and one office manager; 2) Two shifts: two equipment operators; 3) Three shifts: two control room operators, four auxiliary operators, one instrument technician, two mechanics and one maintenance foreman. Salaries and social insurance were included [28]. The public grants considered were that actually in force in Spain. At last, the CO₂ avoided emissions costs were obtained from the actual emissions markets. Finally, NPV were obtained by calculating the annual cash flow of the respective scenario.

COE and CCA calculations were based on the EBTF methodology. The COE was calculated with the IEA procedure, which vary the MWeh price until the specific scenario NPV goes to zero with no public grants considering.

Table 3
Main considered assumptions in viability studies.

Parameter	Unit	Value
Biomass cost	€/t	47.00
Coal cost	€/t	65.00
Electricity price	€/MWeh	57.75
Discount rate	%	10
Inflation rate	%	2
First year operation	h	6400
Rest of lifetime operation	h	8000
Operating lifetime	Years	25
Labour costs	M€/years	3.58
Public grants, coal	€/MWeh	75.00
Burn grants, coal	€/t	10.00
Public grants, biomass	€/MWeh	53.82
CO ₂ emissions market	€/tCO ₂	10.00

The CCA was calculated as follows:

$$CCA \left[\frac{\text{€}}{\text{kg}_{CO_2}} \right] = \frac{(COE)_{co2,cap} - (COE)_{ref}}{\left(\text{kg}_{CO_2} \cdot \text{kWeh}^{-1} \right)_{ref} - \left(\text{kg}_{CO_2} \cdot \text{kWeh}^{-1} \right)_{co2,cap}} \quad (2)$$

where CO_{2,cap} was the studied CO₂ capture power plant “ref” referred to a reference power plant without capture [22]. Following the IEA methodology, CCA was obtained with no consideration of CO₂ transport and storage.

2.2.3. On the sensitivity analysis

The objective of the sensitivity analysis was to analyse the influence of the more uncertainly parameters affecting to industrial projects viability on NPV variation values. In the present study, a 50% of biomass co-firing level was chosen as the feedstock of the power plants as it was considered to be a compromise value between the use of biomass and the profitability of coal plants.

The selected parameters to be analysed were the biomass price, the coal price, the labour costs, the inflation rate, the electricity price, the CO₂ market price, the biomass public grants and the coal public grants. The reference value of each parameter was that used for obtaining the NPV and COE value in the viability studies. A variation of this reference value between the 80% and 120% of the reference one was used to study the impact of these factors on NPV and COE variations. To make conclusions more representative, the selected parameters were varied individually.

Finally, a Monte Carlo simulation was carried on with the more interesting power plant in terms of the scale-up effect and the results of sensitivity analysis. Monte Carlo simulation provided information to optimize the co-firing level in terms of the lowest COE.

3. Results and discussion

3.1. Technical simulations

A biomass co-firing level of 50% was used to describe the technical simulations and the economic results. The effect of the different biomass co-firing levels will be discussed in the viability studies.

The main characteristics of several processes streams of the power plants were provided in Table 4. The gross power ratios of the power plants were, as follows: 460MWe/300MWe: 1.53, 300MWe/140MWe: 2.14 and 460MWe/140MWe: 3.29. If the combustor outlet mass flow streams are compared, it can be established the following ratios: 460MWe/300MWe: 1.51, 300MWe/140MWe: 1.90, and 460MWe/140MWe: 2.86. The correlation between the increasing of the combustor outlet mass flow and the gross power ratio increasing could be represented by a concave increasing exponential function as it was shown in Fig. 4. This was the single most striking observation to emerge from the data comparison when, in general, extensive variables were compared: the scale-up effect. In this case, an increasing of 53.3% (300–460), 114.3% (140–300) and 228.6% (140–460) of the gross power plants produced a mass flow increasing of 50.6%, 90.0% and 186.2% respectively.

As a result, the scale-up of the proposed oxy-combustion power plants was made the most and, consequently, more interesting, for higher scale-up ratios. More analysis on the current topic will be discussed on the viability studies.

Table 4

Main characteristics of several streams of the power plants for a selected biomass co-firing level of 50%.

↓ Stream	Flowrate (kg/s)			Temperature (°C)			Pressure (bar)		
	140	300	460	140	300	460	140	300	460
Power (MWe) →									
[1]	5.97	12.80	19.63	538.15	538.15	538.15	12.25	12.25	12.25
[4]	5.16	11.06	16.97	440.73	440.73	440.73	27.48	27.48	27.48
[5]	4.27	9.14	14.02	352.96	352.96	352.96	5.41	5.41	5.41
[6]	81.93	175.56	269.19	352.96	352.96	352.96	5.41	5.41	5.41
[8]	4.28	9.17	14.07	271.52	271.52	271.52	2.30	2.30	2.30
[13]	3.69	7.90	12.11	192.65	192.65	192.65	0.90	0.90	0.90
[16]	287.90	547.10	823.92	1109.3	1120.81	1078.34	1.00	1.00	1.00
From HP	97.33	208.57	319.81	358.46	358.56	358.46	51.42	51.42	51.42
From SC	115.00	246.44	377.87	131.15	130.18	129.78	290.00	290.00	290.00
[26]	3.95	8.46	12.98	107.23	107.23	107.23	0.27	0.27	0.27
[30]	115.00	246.44	377.87	25.00	25.00	25.00	12.00	12.00	12.00
[35]	323.92	642.10	852.74	515.36	427.12	479.57	1.00	1.00	1.00
[45]	70.01	150.02	230.04	32.90	32.90	32.90	0.05	0.05	0.05
[46]	8.76	18.77	28.78	414.98	414.98	414.98	81.62	81.62	81.62
[57]	73.96	158.49	243.51	32.00	32.00	32.00	0.05	0.05	0.05
[59]	106.24	227.67	349.09	358.46	358.46	358.46	51.42	51.42	51.42

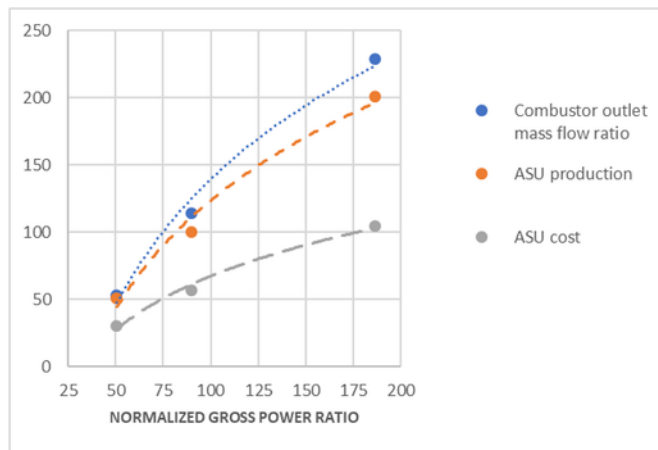
**Fig. 4.** Scale-up effect trend for different representative variables.

Table 5 presented the main technical simulations results. These results can be divided into electric, material and plant component results.

The specific heat provided to water in 460MWe plant heat exchangers shown in Fig. 2 was 7428.2 kJ/kWh. This value was close to 7133,1 kJ/kWh reported in literature by other authors [18] and that obtained by authors in a previous work [10].

Gas compositions were, in 140 MWe, 300 MWe and 460 MWe, 0.029, 0.024, 0.028 for O₂, 0.253, 0.264, 0.265 for H₂O, 0.713, 0.707, 0.703 for CO₂ and 0.004 in all cases for SO₂. Near 70% of gases were CO₂ and 25% were H₂O as it was found in previous works with wet flue gas recycle [18,19]. In addition, excess O₂ in the flue gas (downstream of the boiler) was less than 4% [10,13]. However, the SO₂ amount production resulted to be high enough to be necessary the installation of a DeSOx unit in system [4].

The penalty for electric production by oxy-combustion was mainly produced because: 1) the needing of CO₂ compression previously to storage, 2) the pumping of the water refrigeration system up to the refrigeration tower and 3) the power needing of the ASU [13,21,29,30]. This auxiliary power was 12.3%, 10.7% and 10.1% in 140MWe, 300MWe and 460MWe respectively. Once again, the scaling was more interesting up to 460 MWe, but the impact of the scaling-up was higher in 140–300 than in 300–460 escalation. If auxiliary powers results are projected to a 800 MWe power plant, a value of

Table 5

Main simulation results of the three gross power proposed plants for a selected biomass co-firing level of 50%.

Factor	Unit	140 MWe	300 MWe	460 MWe
Main electric results				
Gross power output	MWe	140.0	300.0	460.0
Auxiliary power	MWe	-17.2	-32.2	-46.6
Net power output	MWe	122.8	267.8	413.4
Main material balances				
Raw material inlet	kg/s	25.1	50.2	75.6
CO ₂ for capture	kg/s	29.2	52.2	80.2
Water on Rankine cycle	kg/s	115.0	246.4	319.9
ASU production (O ₂)	kg/s	32.6	65.2	98.2
Plant component				
Raw material crusher	kWe	85.2	170.5	256.8
Air Separation Unit	kg/s O ₂	32.6	65.2	98.2
Combustor+Evap+Fuel dryer	kg/s H ₂ O	115.0	246.4	319.9
Economizers	m ²	1019.0	2888.0	4518.4
Flue gas heater	m ²	408.4	776.9	1173.5
Oxygen heater	m ²	2.1	5.3	8.1
Nitrogen heater	m ²	9.3	22.6	34.5
DeSOx Unit	kg/s SO _x	0.4	0.7	1.1
Dryer & Compression unit	kg/s CO ₂	29.2	52.2	80.2
Electrostatic precipitator	kWe	160.4	299.1	408.5
Water refrigeration system	GJ/h	604.0	1294.4	1984.7
Steam condenser	m ²	1.8	3.9	6.0
High temperature heaters	m ²	65.2	139.1	212.9
Water pump	kWe	1364.1	2679.6	3955.2
Low temperature heaters	m ²	1319.9	2822.1	4323.4
Condensate pump	kWe	151.5	306.3	458.6
Deareator	kg/s H ₂ O	115.0	246.4	319.9
Condenser	GJ/h	604.0	1294.4	1984.7
HP multistage turbine	MWe	40.9	87.7	134.4
IP multistage turbine	MWe	49.6	106.2	162.9
LP multistage turbine	MWe	49.5	106.1	162.7

8.2% is obtained. This value was in accordance with that obtained by Ali et al. [16] for a 800 MWe power plant but it differed with the study of Yan et al. [31]. However, it was consistent with that obtained by authors in a previous work [10].

The main material balances followed the same trend that of extensive variables previously described. Naturally, it was necessary more raw material inlet and ASU production in the plant with the highest electricity production. Consequently, water in Rankine cycle and CO₂ produced for storage followed the same sense.

In 460 MWe power plant, the specific water mass flow in Rankine cycle was 2503.6 kg/MWh. A value of 2630.1 kg/MWh was previously obtained by Kotowicz et al. [18] in a simulation of a 460 MWe power plant. In addition, Janusz-Szymanska and Dryjanska reported a

value of 2586.1 kg/MWh in a study of a 600 MWe power plant. These findings contribute to validate the technical results obtained in this work.

At last, Ali et al. [16] found a specific flue gas of 693.5 kg/MWh in a recent study, not so far (10%) than that obtained in this work (627.7 kg/MWh).

The plant components results were indicated by a representing variable of each one. If they are analysed by comparing the same equipment in the different power plants, the correlation between the representative variable and the gross power increasing could be represented by a concave increasing exponential function, in accordance with previous results found in Table 4. This trend was shown, for a representative variable, in Fig. 4.

If the different equipment are compared for a specific power plant, another discussion could be performed. If heat exchangers are compared in the same power plant, 140MWe for example, the highest exchange area belonged to the low temperature heaters (as a whole) of the Rankine cycle, as they were designed by the use of a relative low-temperature water in heat integration. As evaporator cost was obtained as a whole with combustor, the area value was not presented in Table 5. However, this heat exchanger resulted to be the highest exchanger area in Aspen Plus[®] simulations due to its thermal exchange value as it was expected [22]. The condenser result was expressed as the thermal exchange value because of the costs data sources.

Water pumping had the highest power need in the unit located after deaerator. This equipment need was higher than that of condensate pump due to the water mass flow and the outlet pressure of both systems as it was presented in Table 4 and it was previously explained in the followed methodology. Finally, the IP turbine was found to be the main power generator. These results were consistent with that reported by other authors [32,33].

3.2. Economic viability studies

Two parts were included in the economic viability studies. First, economic results were analysed and compared. At last, the viability parameters were discussed.

3.2.1. Economic results

The main economic results were presented in Table 6. It is important to note that Table 6 was an only sample representation of the rest of the study (50% of biomass co-firing level).

By comparing the proposed power plants results, it was observed that every plant component cost was in a behaviour accordance with the technical results previously discussed: the correlation between the increasing of the plant component costs and the gross power increasing could be represented by a concave increasing exponential function. This trend was shown, for a representative variable, in Fig. 4.

The highest values presented in Table 6 corresponded to the combustor, the turbines and the cryogenic O₂ production. This finding was previously corroborated in other studies [22,23,33,34]. For a better analysis, a TEC pool distribution by process areas for a selected 300MWe power plant with a biomass co-firing level of 50% was presented in Fig. 5.

On this question, this study found the combustor and evaporator to be the highest relative equipment costs up to 40.9% of TEC. This result was in agreement with that reported by Seltzer and Robinson (38.9%) and the US Department of Energy [23,35]. Heat recovery costs represented a 5.7% of compression costs. This value was expected to be below 5% according to Fu and Gundersen [34] but it was in agreement with other reports [23,35]. Turbines represented a 21.9% of TEC and ASU represented no more than 16.5%. These

Table 6

Main economic results of the power plants for a selected co-firing level of 50%.

Factor	140 MWe	300 MWe	460 MWe
Plant component, (M€)			
Raw material crusher	0.15	0.24	0.32
Air Separation Unit	22.82	35.81	46.74
Combustor+Evap+Fuel dryer	52.20	89.00	106.82
Economizers	0.41	0.84	1.14
Flue gas heater	0.15	0.23	0.30
Oxygen heater	0.004	0.007	0.009
Nitrogen heater	0.01	0.02	0.03
DeSOx unit	7.19	11.75	15.65
Dryer & Compression unit	12.62	18.95	25.62
Electrostatic precipitator	3.34	5.17	6.43
Water refrigeration system	1.26	2.15	2.96
Steam condenser	0.003	0.006	0.007
High temperature heaters	0.06	0.09	0.13
Water pump	0.74	1.18	1.55
Low temperature heaters	0.41	0.69	0.93
Condensate pump	0.13	0.29	0.29
Deaerator	0.04	0.06	0.09
Condenser	1.60	2.73	3.69
HP multistage turbine	8.50	14.48	19.54
IP multistage turbine	9.72	16.57	22.35
LP multistage turbine	9.71	16.55	22.32
Total Equipment Costs, TEC	131.08	216.88	276.92
Global results, (M€)			
Total Equipment Costs, TEC	131.08	216.88	276.92
Total Direct Costs	304.38	503.60	643.01
Total Indirect Costs	181.68	300.60	383.81
Working Capital	108.14	178.93	228.46
Total Capital Investment, TCI	725.28	1200.00	1532.21
Specific Investment (M€/MWe)	5.18	4.00	3.33
Utilities, (M€/year)			
Process compressed air	0.22	0.45	0.67
Air Separation Unit	6.84	12.76	18.45
Electricity	0.81	1.59	2.34
Refrigeration to 32 °C	9.77	11.06	13.23
Ash and gypsum disposal	1.26	5.44	8.20
Limestone	1.10	2.21	3.33
Total utilities (M€/year)	20.00	32.22	46.22

findings were consistent with those of Xiong et al. [33]. Finally, coal and biomass preparation represented a residual value in agreement with actual literature.

If TCI is observed, the obtained values were in accordance with technical results and with previous similar industrial plants [23,33].

Another important factor to be evaluated was the power plants specific investment. The values shown in Table 6 could be represented by a convex decreasing exponential function with good accuracy ($r^2=0.99$). This also accorded with earlier observations reported by Campanari et al. [32] and other authors [17,36]. The US Department of Energy [23] reported a reference value of 2.47 M€/MWe in a 679.6 MWe (gross) supercritical PC with CO₂ capture. If specific investment results given in Table 6 are projected for a 679.6 MWe (gross) power plant, it could be obtained a value of 2.43 M€/MWe, according with the reference worth.

Finally, Table 6 presented the utilities cost for each power plant. Water Rankine refrigeration and ASU consumption were found to be the main causes of utilities worth. ASU consumption has been found as the main inconvenient to implement oxy-combustion technology at industrial scale nowadays [29]. Utilities values trend were in accordance with the complexity of power plant considered.

3.2.2. Viability studies

The NPVs were presented in Fig. 6 while the COE and CCA obtained values were shown in Fig. 7.

If NPVs are compared in the three power plants, it can be observed that only a gross power plant of 460MWe production have a

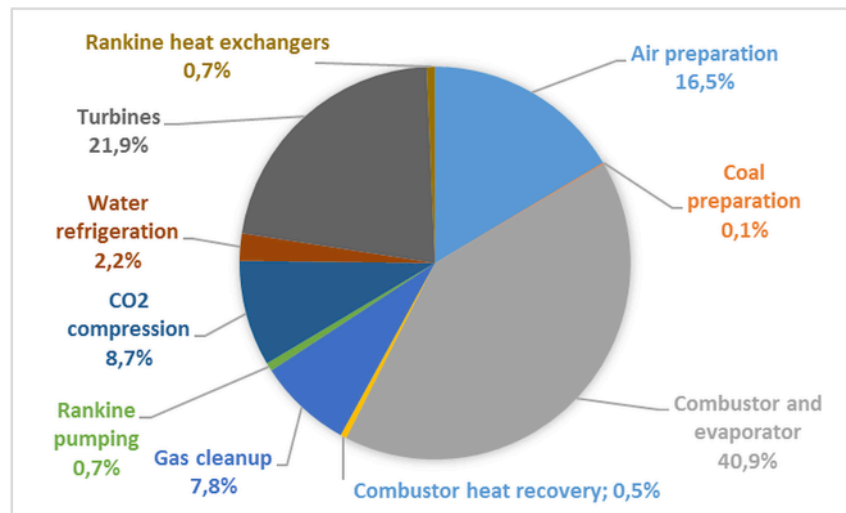


Fig. 5. TEC pool distribution by process areas for a selected 300MWe power plant with a biomass co-firing level of 50%.

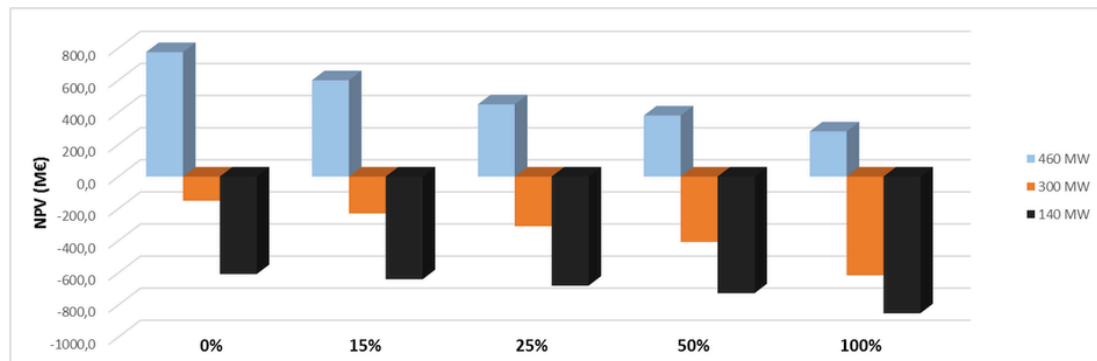


Fig. 6. NPV for different biomass co-firing level in each power plant studied.

positive viability with the main assumptions presented in Table 2. In addition, as biomass co-firing level rises, NPV decreases by a convex exponential function. This finding was in agreement with the technical and economic results previously observed. As it was shown in Table 1, biomass has lower calorific value than coal. In other words, more biomass in the combustor implied a higher size of the combustor area equipment. The lower calorific value also implied more amount of raw material to produce the same gross power electric production. This situation caused a more CO₂ production when biomass co-firing level was higher and, hence, a higher compression power needs and higher exchange area in heat exchangers because the more absorbance that CO₂ caused in the flue gas [12]. In addition, more biomass in the combustor produced a more difficult ash to be separated in the electrostatic precipitator. Hence, a higher power in this equipment was required. All these situations implied a higher capital investment and then, lower profitability. Finally, as biomass public grants were lower than that for coal, cashes flows were reducer than that with more coal in the combustor in every year of plant life. These were the main reasons why NPV reduced by a convex exponential function with biomass co-firing level increase.

The NPV was a parameter based on the economic conditions of the country in which the industrial project is studied. These conditions included public grants and market labour or utilities costs. These were the reasons why it was not possible to make a direct comparison between different power plants found in bibliography without

taking this item into account. The US Department of Energy, towards the Clean Coal Power Initiative, promote the CCS technologies with a public grant from the federal government of 5%–18% of total project cost. In addition, other electric and financial policies are considered [37]. The UK provides a strong line of government funding and support. It reaches the 30% of the plant project budget. In addition, it has been established a CCS Cost Reduction Task Force and a new electric market regulation in order to make CCS plants competitive [38]. With US or UK incentives, all oxy-combustion power plants studied in this work would have a positive viability. However, the lower Spanish incentives made only long size oxy-combustion power plants had a positive viability.

The COE and CCA values did not depend on the policy of the country government. For this reason, they are better representative parameters to compare different power plants studies previously found in bibliography. Fig. 7 a showed COE values between 101 and 129 €/MWh for the 460 MWe plant. These results were slightly higher than that reported by other authors in similar power plants size [29,39,40] but they were in accordance with that reported by Pettinau et al. and the NREL [41,42]. In addition, Skorek-Osikowska et al. reported a value of 108.4 €/MWh in a 460 MWe power plant with a cryogenic air separation [43]. The COE was higher in smaller size power plants. Fig. 7 b showed CCA values between 71 and 90 €/t_{CO2} in the 460 MWe power plant. These results were also higher than various previously found in literature but in agreement with that reported

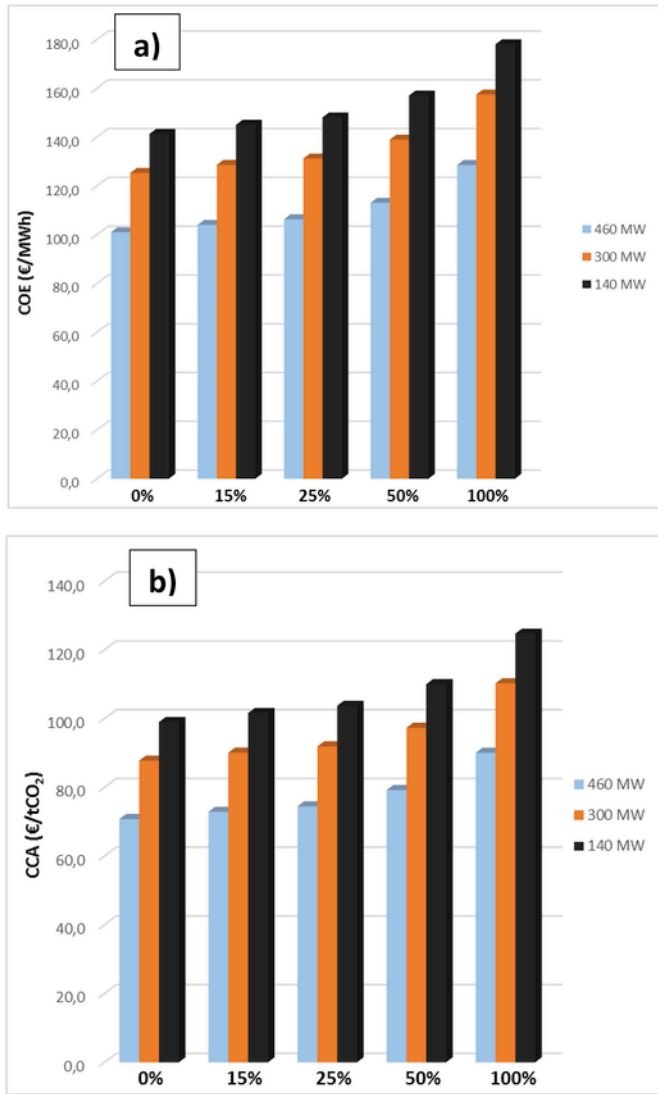


Fig. 7. COE (a) and CCA (b) for different biomass level co-firing in each power plant studied.

by other authors [17,44]. This behaviour can be explained because CCA values are obtained by considering the COE project values. In addition, CCA results could reach the value of 125 €/tCO₂ depending on the plant size and the biomass co-firing level factor. The behaviour of CCA with these two parameters were the same than that previously reported as it was expected and it was previously described by other authors [40]. Both, COE and CCA, and the biomass co-firing level values could be approximate by an increasing exponential function. Reasons were the same that were previously explained in NPV behaviour if it was considered that lower profitability implies higher COE and CCA. However, the slope of the function was lower than that obtained in NPV comparisons. This was caused by the non-considering public grants when COE and CCA were calculated.

In order to improve the study of the scale-up effect, Table 7 presented the specific NPV and COE variations for each biomass co-firing level in the two proposed scale-up situations.

If results about NPV are analysed, it can be observed that the 140–460 MWe scale-up produced a higher NPV variation (2.78–4.32 M€/MWe) than that of 140–300 MWe (1.47–2.86 M€/MWe). In addition, NPV rose in both cases. These results were consistent with

Table 7
Effect of the plants scale-up on NPV and COE variations (M€/MWe).

Scaling	Biomass co-firing level				
	0%	15%	25%	50%	100%
140 MWe-300 MWe					
NPV	2.86	2.56	2.31	1.99	1.47
COE	-0.100	-0.103	-0.105	-0.113	-0.129
140 MWe-460 MWe					
NPV	4.32	3.77	3.31	3.09	2.78
COE	-0.126	-0.128	-0.130	-0.138	-0.155

that reported in the technical results. It is well known that plants scaling produces a better economic balance because of the more yield obtained in every plant equipment or component and, consequently, lower unit production costs. In addition, public grants were higher as plant size increased. Both factors pointed to a better plant profitability in higher scale-up situations.

If biomass co-firing level is observed, it can be shown that the more biomass amount in combustor, the less specific NPV increase by the same scaling factor. This was caused by the less role than public grants play at higher biomass co-firing levels because its lower values.

When COE is observed, it can be seen the opposite trend than that described in NPV case, as it was expected. This behaviour was also lighter than that observed in NPV because the no considered public grants in calculations.

In order to improve the study of the biomass co-firing level, Table 8 presented the specific NPV and COE variations for each proposed level in the three power plants size studied.

If NPV variations are observed, the same conclusions about how biomass amount affected plants viability could be obtained. The exponential trend towards a 100% of biomass content was mainly due to the less public grants of biomass than coal but it was also explained because the higher capital investment and utilities needed with a higher biomass co-firing level. The same effect could be seen by comparing the NPV variation differences in the different power plants size with the same biomass scaling level. In the fifteen scenarios, NPV variation can be found in the interval (-0.23,-1.75) M€/MWe.

The COE had the opposite behaviour than NPV. In addition, a lower impact of biomass scaling on COE variation was obtained because the no considered public grants in calculations, as it was previously observed. The low impact of the biomass co-firing level on the NPV and COE variations was caused by the lower importance that biomass co-firing level had in flow cashes than the scale-up factor produced. However, it could be identified some couple values with similar effects, as absolute value, on NPV variations, such as the

Table 8
Effect of the biomass co-firing level on NPV and COE variations (M€/MWe).

Power	Biomass scaling			
	0-15%	0-25%	0-50%	0-100%
140 MWe				
NPV	-0.23	-0.52	-0.85	-1.75
COE	0.027	0.048	0.113	0.263
300 MWe				
NPV	-0.26	-0.53	-0.86	-1.55
COE	0.011	0.020	0.046	0.107
460 MWe				
NPV	-0.38	-0.71	-0.86	-1.07
COE	0.007	0.012	0.026	0.060

140–300 MWe scale-up effect with 100% of biomass and the scaling of 0–100% biomass at 300 MWe.

An increasing of COE and CCA values when changing the feedstock from coal to lignocellulosic biomass was also observed by Al-Qayim et al. They reported a COE value of 88.6 €/MWh and a CCA value of 52.3 €/t_{CO2} in a 650 MWe coal oxy-combustion power plant. These values rose to 165.3 €/MWh and 90.6 €/t_{CO2}, respectively, when the same power plant was fed only with lignocellulosic biomass. The increasing values obtained in this work were lower than that obtained by Al-Qayim et al. but they were in accordance with that observed by authors in a previous work with the same raw materials [10].

3.3. Sensitivity analysis

In this study, a 50% of biomass co-firing level was selected and diverse parameters were studied for the three power plants size.

The results of the sensitivity analysis were shown in Fig. 8 (a, b, c). The slope of all figures was higher in the highest size plants, in order: 460 MWe > 300 MWe > 140 MWe. This trend was in accordance with that obtained in the technical and viability studies. It could be explained by the higher impact that prices, costs and grants produced in flow cashes of high electric plants production.

Variables with a positive impact on NPV values were, in order of importance: electric price > public coal grants > public biomass grants > CO₂ market price. This results were consistent with previous studies [41]. However, the variables with a negative impact on NPV values were, in order: inflation rate > coal price > biomass price > labour costs. As a result, the stability parameters were more important, in order: electric price > coal grants > inflation rate > coal price > biomass price > biomass grants > CO₂ market price > labour costs. This trend was also observed by Cormos before [45]. This classification established a priority in stability of parameters needed for making bio-CCS more attractive to potential investors. The electric price was found to be the most important factor. An increasing in 10% of the electric price could produce a NPV rises of 261.7 M€ in 460 MWe plant, reaching a 69% of increment in the NPV. This is the reason of importance of stability in international markets. However, the electric price impact on 140 MWe plant reduced to a 11% of NPV variation.

Public grants were also a decisive factor to make promoters to be confidence in implementing these technologies. In 460 MWe plant, an increment of 10% of coal grants could produce an increment of 52% of NPV. However, an increment of 10% of biomass grants produced a variation of 23% in NPV. In 140 MWe plant, both NPV increments were 8% and 4% respectively.

On the other side, an increasing of 10% of inflation rate could produce a reduction of 24% on NPV in 460 MWe plant. This value decreased to a 7% in 140 MWe power plant. Otherwise, an increasing of 10% of labour costs could reduce the NPV by a 3% in 460 MWe plant, while this reduction can be established in no more than 1% in 140 MWe plant. As a result, 460 MWe power plants needs more stability in several key aspects, such as government legislation, market prices, international agreements or energetic policies than 140 MWe power plants. Consequently, higher power plants are more risky than smaller ones. This discussion focused to the conclusion that a 300 MWe power plant could be a compromise power value between the scale-up effect and the risk observed in sensitivity analysis.

Finally, in order to optimize the co-firing ratio value, 50 simulations in a 300 MWe power plant were carried on by obtaining the COE with a variation of the co-firing ratio in a Monte Carlo simula-

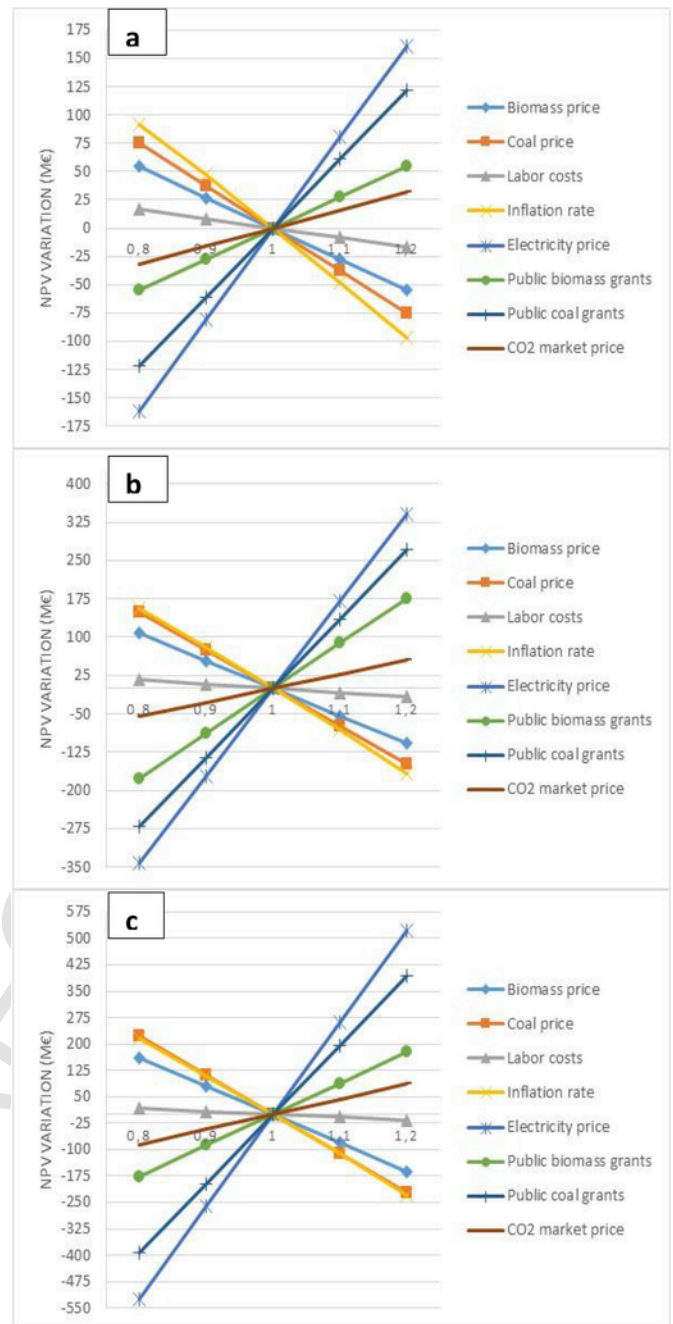


Fig. 8. Results of sensitivity analysis on NPV for a) 140 MWe, b) 300 MWe and c) 460 MWe.

tion. The results were presented in Fig. 9. At view of Fig. 9, the COE can be estimate as 141.1 ± 5.1 €/MWh with a 95% of confidence. The interval limits belong to a co-firing ratio of 40 and 72% when results were interpolated in Fig. 7 values. In addition, COE vs. co-firing ratio slope rises from 0.22 (0–15%), 0.26 (0–25%), 0.31 (0–50%) to 0.37 (0–100%). A compromise solution can be achieved by selecting a co-firing ratio between 25 and 50%. As a result, the more interesting bio-CCS power plants construction are 300 MWe power plants with 40–50% biomass co-firing level. These plants can be located in a compromise point of biomass using and plant risks.

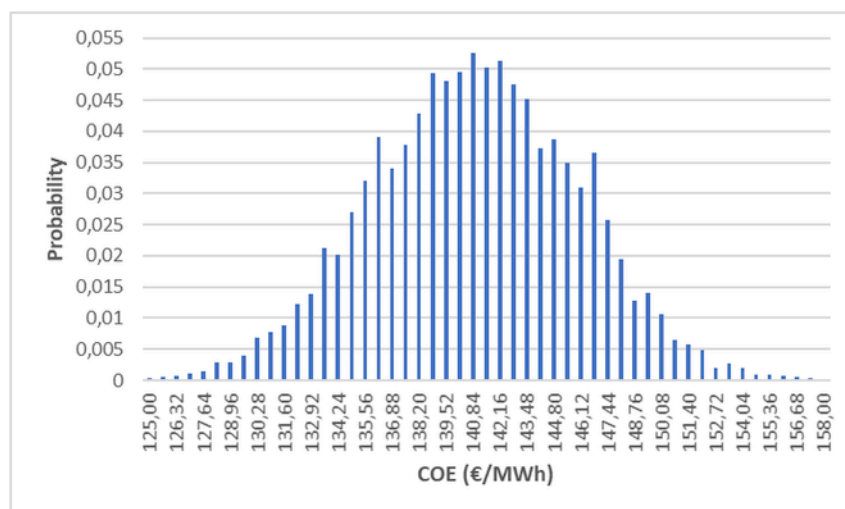


Fig. 9. Monte Carlo results representation of the 300 MWe power plant.

4. Conclusions

Some interesting conclusions have been reached in this work. First, 300 MWe and 140 MWe coal-corn-rape oxy-combustion power plants need between (4.9–20.4) and (42.5–59.6) €/MWh additional public grants, respectively, depending on the considered biomass co-firing level to reach positive viability. Second, the use of corn and rape as biomass raw material with coal increases the COE by (0.007,0.263) M€/MWe. Third, the scale-up of oxy-combustion power plants results to be more relevant than a reduction of the biomass co-firing level in cash flow terms. The scale-up effect can reach 4.32 M€/MWe in (140–460) MWe while the biomass reduction only reaches 1.52 M€/MWe in 140 MWe power plant (all values in Spanish conditions NPV variations terms). Fourth, the reduction of oxy-plants viability by using of biomass as raw material can be compensated by an increasing of the designed scale-up of such plants. For example, the 140–300 MWe scale-up effect with 100% of coal-rape can compensate the use of only biomass as raw material in 300 MWe power plants. Fifth, the stability parameters are more important in Spanish markets, in order: electric price > coal grants > inflation rate > coal price > biomass price > biomass grants > CO₂ market price > labour costs. Sixth, 460 MWe power plants needs more stability than 140 MWe power plants due to the impact than some usually instability variables cause in cash flows. However, the need of stability of raw material and electricity markets were found very important in all cases. Finally, the more interesting bio-CCS power plants construction are 300 MWe power plants with 40–50% lignocellulosic biomass co-firing level. These plants can be located in a compromise point of biomass using and plant risks. The positive viability could be reached by getting an extra-grant of 10€/MWh by an increasing of the European Union funds used for climate change reduction.

Acknowledgements

This research did not receive any specific grant from funding agencies in the public, commercial, or not-for-profit sectors. Authors thanks the assistance of University of Oviedo (Spain) Chemical Engineering Department in the implementation of the technical simulations of this study.

References

- [1] UNFCCC, Earth information day 2016, 2016 <http://unfccc.int/science/streams/items/9949.php>, Accessed 30 December 2016.
- [2] UNEP, Sustainable innovation forum at COP22, 2016 <http://www.cop22.org/>, Accessed 30 December 2016.
- [3] European Commission, Official journal of the European union, 2009 <http://eur-lex.europa.eu/oj/direct-access.html?locale=en>, Accessed 20 October 2016.
- [4] Spanish Government, Official journal of the Spanish government, 2011, boe.es Accessed 20 October 2016.
- [5] J. Kemper, International journal of greenhouse gas control biomass and carbon dioxide capture and storage: a review, 40 (2015) 401–430, <https://doi.org/10.1016/j.ijggc.2015.06.012>.
- [6] A.A. Rentizelas, J. Li, Techno-economic and carbon emissions analysis of biomass torrefaction downstream in international bioenergy supply chains for co-firing, Energy 114 (2016) 129–142, <https://doi.org/10.1016/j.energy.2016.07.159>.
- [7] J.C. Abanades, B. Arias, A. Lyngfelt, T. Mattisson, D.E. Wiley, H. Li, et al., Emerging CO₂ capture systems, Int J Greenh Gas Control 40 (2015) 126–166, <https://doi.org/10.1016/j.ijggc.2015.04.018>.
- [8] P. Ashworth, S. Wade, D. Reiner, X. Liang, Developments in public communications on CCS, Int J Greenh Gas Control 40 (2015) 449–458, <https://doi.org/10.1016/j.ijggc.2015.06.002>.
- [9] N. Perrin, R. Dubettier, F. Lockwood, J.P. Tranier, C. Bourhy-Weber, P. Terrien, Oxycombustion for coal power plants: advantages, solutions and projects, Appl Therm Eng 74 (2015) 75–82, <https://doi.org/10.1016/j.applthermaleng.2014.03.074>.
- [10] R. López, C. Fernández, O. Martínez, M. Sánchez, Techno-economic analysis of a 15MW corn-rape oxy-combustion power plant, Fuel Process Technol 142 (2016) 296–304, <https://doi.org/10.1016/j.fuproc.2015.10.020>.
- [11] International Energy Agency, Focus on clean coal, Focus Clean Coal, 2006.
- [12] R. López, C. Fernández, J. Cara, O. Martínez, M.E. Sánchez, Differences between combustion and oxy-combustion of corn and corn-rape blend using thermogravimetric analysis, Fuel Process Technol 128 (2014) 376–387, <https://doi.org/10.1016/j.fuproc.2014.07.036>.
- [13] R. Stanger, T. Wall, R. Spörl, M. Paneru, S. Grathwohl, M. Weidmann, et al., Oxyfuel combustion for CO₂ capture in power plants, Int J Greenh Gas Control 40 (2015) 55–125.
- [14] R. López, C. Fernández, O. Martínez, M.E. Sánchez, Modelling and kinetics studies of a corn-rape blend combustion in an oxy-fuel atmosphere, Bioresour Technol 183 (2015) 153–162, <https://doi.org/10.1016/j.biortech.2015.02.040>.
- [15] Gas Natural Fenosa, Technical paper of Unión Fenosa power plant. La Robla, Spain, 2016.
- [16] U. Ali, C. Font-Palma, M. Akram, E.O. Agbonghae, D.B. Ingham, M. Pourkashanian, Comparative potential of natural gas, coal and biomass fired power plant with post-combustion CO₂ capture and compression, Int J Greenh Gas Control 63 (2017) 184–193, <https://doi.org/10.1016/j.ijggc.2017.05.022>.
- [17] R.T.J. Porter, M. Fairweather, C. Kolster, N. Mac Dowell, N. Shah, R.M. Woolley, Cost and performance of some carbon capture technology options for producing different quality CO₂ product streams, Int J Greenh Gas Control 57 (2017) 185–195, <https://doi.org/10.1016/j.ijggc.2016.11.020>.

- [18] J. Kotowicz, H. Lukowicz, Ł. Bartela, S. Michalski, Validation of a program for supercritical power plant calculations, *Arch Thermodyn* 32 (2011) 81–89, <https://doi.org/10.2478/v10173-011-0033-1>.
- [19] K. Janusz-Szymańska, A. Dryjańska, Possibilities for improving the thermodynamic and economic characteristics of an oxy-type power plant with a cryogenic air separation unit, *Energy* 85 (2015) 45–61, <https://doi.org/10.1016/j.energy.2015.03.049>.
- [20] X. Pei, B. He, L. Yan, C. Wang, W. Song, J. Song, Process simulation of oxy-fuel combustion for a 300 MW pulverized coal-fired power plant using Aspen Plus, *Energy Convers Manag* 76 (2013) 581–587, <https://doi.org/10.1016/j.enconman.2013.08.007>.
- [21] P. Higginbotham, V. White, K. Fogash, G. Guvelioglu, Oxygen supply for oxy-fuel CO₂ capture, *Int J Greenh Gas Control* 5 (2011) S194–S203, <https://doi.org/10.1016/j.ijggc.2011.03.007>.
- [22] DOE/NETL, Cost and performance baseline for fossil energy plants volume 1b: bituminous coal (IGCC) to electricity, 20151, doi:DOE/NETL-2010/1397.
- [23] DOE/NETL, Cost and performance of PC and IGCC plants for a range of carbon dioxide capture, 20111–500.
- [24] D.P. Hanak, D. Powell, V. Manovic, Techno-economic analysis of oxy-combustion coal-fired power plant with cryogenic oxygen storage, *Appl Energy* 191 (2017) 193–203, <https://doi.org/10.1016/j.apenergy.2017.01.049>.
- [25] L. Brickett, U. Netl, CCS cost network 2016 workshop, 2016.
- [26] M. Peters, K. Timmerhaus, R. West, *Plant design and economics for chemical engineers*, fifth ed., 2007.
- [27] Bloomberg, in: <https://www.bloomberg.com/europe>, 2016 Accessed 20 October 2016.
- [28] Eurostat, in: <http://ec.europa.eu/eurostat>, 2016 Accessed 20 October 2016.
- [29] E.S. Rubin, J.E. Davison, H.J. Herzog, The cost of CO₂ capture and storage, *Int J Greenh Gas Control* 40 (2015) 378–400, <https://doi.org/10.1016/j.ijggc.2015.05.018>.
- [30] P. Luckow, E.A. Stanton, S. Fields, B. Biewald, S. Jackson, J. Fisher, et al., Carbon dioxide price forecast, Synap Energy Econ Inc, 20151–39.
- [31] K. Yan, X. Wu, A. Hoadley, X. Xu, J. Zhang, L. Zhang, Sensitivity analysis of oxy-fuel power plant system, *Energy Convers Manag* 98 (2015) 138–150, <https://doi.org/10.1016/j.enconman.2015.03.088>.
- [32] S. Campanari, P. Chiesa, G. Manzolini, S. Bedogni, Economic analysis of CO₂ capture from natural gas combined cycles using molten carbonate fuel cells, *Appl Energy* 130 (2014) 562–573, <https://doi.org/10.1016/j.apenergy.2014.04.011>.
- [33] J. Xiong, H. Zhao, C. Zheng, Thermo-economic cost analysis of a 600MW e oxy-combustion pulverized-coal-fired power plant, *Int J Greenh Gas Control* 9 (2012) 469–483, <https://doi.org/10.1016/j.ijggc.2012.05.012>.
- [34] C. Fu, T. Gundersen, Techno-economic analysis of CO₂ conditioning processes in a coal based oxy-combustion power plant, *Int J Greenh Gas Control* 9 (2012) 419–427, <https://doi.org/10.1016/j.ijggc.2012.05.005>.
- [35] A. Seltzer, A. Robertson, Economic analysis for conceptual design of supercritical O₂-Based PC boiler. Livingston, New Jersey, 2006.
- [36] A. Skorek-osikowska, Ł. Bartela, J. Kotowicz, M. Job, Thermodynamic and economic analysis of the different variants of a coal-fired, 460 MW power plant using oxy-combustion technology, *Energy Convers Manag* 76 (2013) 109–120, <https://doi.org/10.1016/j.enconman.2013.07.032>.
- [37] U.S. National Coal Council, Fossil Forward: revitalizing CCS bringing scale and speed to CCS deployment, 2015.
- [38] U.K. Department for Business-Energy & Strategy, UK carbon capture and storage: government funding and support, November 2015 <https://www.gov.uk/guidance/uk-carbon-capture-and-storage-government-funding-and-support#ccs-cost-reduction-task-for> Accessed 28 December 2016.
- [39] J. Davison, Performance and costs of power plants with capture and storage of CO₂, *Energy* 32 (2007) 1163–1176, <https://doi.org/10.1016/j.energy.2006.07.039>.
- [40] E. Agbor, A.O. Oyedun, X. Zhang, A. Kumar, Integrated techno-economic and environmental assessments of sixty scenarios for co-firing biomass with coal and natural gas, *Appl Energy* 169 (2016) 433–449, <https://doi.org/10.1016/j.apenergy.2016.02.018>.
- [41] A. Pettinau, F. Ferrara, C. Amorino, Techno-economic comparison between different technologies for a CCS power generation plant integrated with a sub-bituminous coal mine in Italy, *Appl Energy* 99 (2012) 32–39, <https://doi.org/10.1016/j.apenergy.2012.05.008>.
- [42] NREL, Equipment design and cost estimation for small modular biomass systems, synthesis gas cleanup, and oxygen separation equipment Task 2: gas cleanup design and cost equipment design and cost estimation for small modular biomass systems, synthesis gas, 20061–117, NREL Rep SR-510-39945.
- [43] A. Skorek-Osikowska, Ł. Bartela, J. Kotowicz, A comparative thermodynamic, economic and risk analysis concerning implementation of oxy-combustion power plants integrated with cryogenic and hybrid air separation units, *Energy Convers Manag* 92 (2015) 421–430, <https://doi.org/10.1016/j.enconman.2014.12.079>.
- [44] A. Bhave, R.H.S. Taylor, P. Fennell, W.R. Livingston, N. Shah, N. Mac Dowell, et al., Screening and techno-economic assessment of biomass-based power generation with CCS technologies to meet 2050 CO₂ targets, *Appl Energy* 190 (2017) 481–489, <https://doi.org/10.1016/j.apenergy.2016.12.120>.
- [45] C.C. Cormos, Oxy-combustion of coal, lignite and biomass: A techno-economic analysis for a large scale Carbon Capture and Storage (CCS) project in Romania, *Fuel* 169 (2016) 50–57, <https://doi.org/10.1016/j.fuel.2015.12.005>.